# In-Situ Gas-Phase Luminescence and Time-of-Flight Mass Spectroscopic Detection of Photofragments during Photochemical Synthesis of Copper Particles from Bis(*tert*-butylacetoacetato)copper

**Jinwoo Cheon*,† and Jeffrey I. Zink*,‡**

Center for Molecular Science and Department of Chemistry, Korea Advanced Institute of Science and Technology (KAIST), Taejon 305-701, Korea, and Department of Chemistry and Biochemistry, University of California, Los Angeles, California 90095

*Received August 11, 1999*

During the 308 nm laser-driven photochemical synthesis of Cu particles from bis(*tert*-butylacetoacetato)copper, gas-phase photogenerated intermediates are identified by luminescence and time-of-flight mass spectroscopies. Pure Cu deposits are obtained as homogeneous, granular 200 nm particles. In the gas phase, luminescent photoproducts are observed and atomic Cu, $Cu_2$, and dissociated ligand are identified spectroscopically. In addition, mass spectroscopy identifies Cu atoms, the dissociated ligand, a monoligated complex, and fragments of the ligands. The implications of the photofragmentation that produces copper atoms and dimers for the laser-assisted production of the Cu deposits are discussed.

## Introduction

For the past decade, photochemical applications for materials synthesis and modification have been widely explored.[1−6] In particular, laser-assisted chemical vapor deposition (CVD) processes have attracted attention for several reasons including selective energy transfer to the organometallic precursor molecules, low-temperature synthesis, and the spatial selectivity and patterning of desired materials.[7−9] There are two general processes responsible for the laser-induced deposition: photolysis in which bond breaking results from the absorption of the laser light by the precursor molecule; photothermal processes in which the heating of the substrate by the laser leads to the thermal decomposition of the precursor. The gas-phase photoreactions that occur are complicated and poorly explored. This paper focuses on the identification of photofragments and the mechanistic aspects of the gas phase photochemistry. The purely gas-phase photolytic decomposition processes of the precursors involved in the vapor deposition are not well understood and need careful mechanistic studies. Under laser-induced CVD conditions, metal−ligand dissociation is possible and photofragments generated during the laser-induced CVD can be identified spectroscopically. Emission of light may be observed, and luminescence spectroscopy can then be used to identify photofragments and assist in the elucidation of the photolytic deposition pathways.[10−15] Time-of-flight mass spectroscopy is important as a complementary tool because it detects nonemitting species.

Copper is an important metal for microelectronics applications, and the CVD of Cu metal has been extensively studied.[16] One of the well-studied CVD precursors is $Cu(hfac)_2$ (hfac = 1,1,1,5,5,5-hexafluoropentane-2,4-dionate); this precursor decomposes when heated in the presence of hydrogen to give high-quality Cu deposits. In contrast, during the photochemical CVD process, fluorine incorporation in the final bulk materials occurs when fluorinated $\beta$-diketonate precursors are used.[17,18] Interestingly, when we examined the gas-phase photoproducts of $Cu(hfac)_2$ by luminescence spectroscopy, diatomic CuF was identified as a major product in the gas phase, suggesting that fluorine contamination of the thin film is generated in the gas phase.[12] Generation of diatomic metal fluoride as photofragments in the gas-phase photolysis of $M(hfac)_2$ (M = Cu, Cr, Ni) has been observed in our recent luminescence spectroscopic studies, and it is suggested that the use of fluorine-containing ligands can lead to fluorine contamination of the final deposits.[19] The presence of fluorine contamination prevents the use of the films in many applications including microelectronic and optical devices.

In this paper, we present the photochemical synthesis of copper deposits and in-situ spectroscopic elucidation of the

† KAIST.
‡ University of California.

(1) Avey, A. A.; Hill, R. H. *J. Am. Chem. Soc*. **1996**, *118*, 237.
(2) Doppelt, P.; Baum, T. H. *MRS Bull.* **1994**, *19*, 41.
(3) Larciprete, R. *Appl. Surf. Sci.* **1990**, *46*, 19.
(4) Lee, E. J.; Bitner, T. W.; Ha, J. S.; Shane, M. J.; Sailor, M. J. *J. Am. Chem. Soc*. **1996**, *118*, 5375.
(5) Bhatia, S. K.; Hickman, J. J.; Ligler, F. S. *J. Am. Chem. Soc*. **1992**, *114*, 4432.
(6) Dressick, W. J.; Dulcey, C. S.; Georger, J. H. Jr.; Calvert, J. M. *Chem. Mater*. **1993**, *5*, 148.
(7) Kompa, K. L. *Angew. Chem., Int. Ed. Engl*. **1988**, *27*, 1314.
(8) Herman, I. P. *Chem. Rev*. **1989**, *89*, 1323.
(9) Eden, J. G. *Photochemical Vapor Deposition*; Wiley: New York, 1992.
(10) Wexler, D.; Zink, J. I.; Tutt, L. W.; Lunt, S. R. *J. Phys. Chem*. **1993**, *97*, 13563.
(11) Chaiken, J.; Casey, M. J.; Villarica, M. *J. Phys. Chem*. **1992**, *96*, 3183.
(12) Talaga, D. S.; Zink, J. I. *Inorg. Chem.* **1996**, *35*, 5050.
(13) Cheon, J.; Talaga, D. S.; Zink, J. I. *J. Am. Chem. Soc*. **1997**, *119*, 163.
(14) Cheon, J.; Zink, J. I. *J. Am. Chem. Chem.* **1997**, *119*, 3838.
(15) Cheon, J.; Talaga, D. S.; Zink, J. I. *Chem. Mater*.. **1997**, *9*, 1208.
(16) *The Chemistry of Metal CVD*; Kodas, T. T., Hampden-Smith, M. J., Eds.; VCH: Weinheim, Germany, 1994.
(17) Izquierdo R.; Bertomeu, J.; Suys, M.; Sacher, E.; Meunier, M. *Appl. Surf. Sci*. **1995**, *86*, 509.
(18) *Laser Chemical Processing for Microelectronics*; Ibbs, K. G., Osgood, R. M., Eds.; Cambridge University: Cambridge, U.K., 1989; pp 37−41.
(19) Talaga, D. S.; Hanna, S. D.; Zink, J. I. *Inorg. Chem.* **1998**, *37*, 2880.

10.1021/ic990962a CCC: $19.00 
Published on Web 00/00/0000 PAGE EST: 3.9

photofragmentation processes from a volatile, air-stable, and fluorine-free precursor $Cu(MeCOCHCOOBu^t)_2$.[20] While many metal $\beta$-diketonate complexes with nonfluorinated ligands such as acetylacetonate (acac) have inadequate vapor pressure for the CVD process, the keto-ester type precursor used here is volatile even without fluorines. Recently, thermal CVD of this type of precursors has been shown to give outstanding quality Cu thin films at low temperatures.[21] Here, we use gas-phase luminescence and time-of-flight mass spectroscopies during the laser CVD process to monitor the laser-driven fragmentation pathways. These two analytical tools are complementary methods of obtaining real time information on the active species present. Interestingly, the deposits consist of homogeneous spherical particles, and we characterize their purity and crystallinity. This study is one of the few demonstrations of the simultaneous utilization of a laser not only for the initiation but also for in-situ characterization of materials synthesis.

## Experimental Section

**Materials and General Methods.** The precursor molecule cupric *tert*-butylacetoacetate [$Cu(baa)_2$], $Cu(MeCOCHCOOBu^t)_2$, was prepared by following literature methods.[20] After recrystallization from $CHCl_3$ and characterization by $^1H$ NMR and mass spectroscopy (EI), it was used for CVD and gas-phase spectroscopic experiments. The deposits were characterized by surface analytical methods. X-ray powder diffraction (XRD) patterns were acquired using Cu K$\alpha$ radiation with a power supply of 40 kV and 30 mA. Scanning electron micrographs were obtained on a Cambridge Stereo Scan 250 instrument. X-ray photoelectron spectra were obtained with a 15 kV, 400 W Al K$\alpha$ radiation source (1486.6 eV) at an operation pressure of ca. $10^{-9}$ Torr. The surfaces of the films were cleaned by $Ar^+$ sputtering of the films for 3−5 min (corresponding to roughly 20−30 nm in depth).

**Luminescence Spectroscopy.** Luminescence experiments are carried out in an evacuated stainless steel 6-way cross with synthetic fused silica windows. A sample of the precursor is placed in the sample chamber and is leaked into the photolysis chamber with a needle valve. The gas-phase luminescence spectra are obtained by exciting the gas-phase sample with 308 nm radiation from a XeCl excimer laser (Lambda Physik EMG 201 MSC). The pulse energy used for excitation of the CVD precursors is approximately 3 mJ, and the resulting fluence is typically ~3 MW/cm$^2$. The focused output of the laser excites the gaseous sample and the emitted light is collected at right angles and directed into a 0.32 m single monochromator (JY HR320) where it is dispersed by a 300 or a 600 groove/mm holographic grating and detected by an UV intensified diode array detector (EG&G Princeton Applied Research OMA3 1024 × 1). Details of this experimental setup were described elsewhere.[12]

**Time-of-Flight Mass Spectroscopy.** The TOF mass spectrometer was constructed and assembled at UCLA. The precursor is admitted to the high-vacuum chamber via a supersonic jet. The base pressure of the chamber is always less than $10^{-5}$ Torr. The photoionization for mass spectroscopy is carried out in a stainless steel cube (30 cm edge length) with quartz windows evacuated to $10^{-7}$ Torr with a 12 in. diffusion pump fitted with a water-cooled baffle. A general valve series 9 high-speed solenoid valve (0.5 mm orifice) sends a 0.2 ms pulse of the sublimed sample in the carrier gas with a backing pressure of about $10^3$ Torr downward to intersect the incoming photons at 90°. The distance between the orifice and the laser beam is 5 cm. The XeCl excimer laser (Lambda Physik EMG 201 MSC) provides 308 nm photons required for photolysis. The beam is focused by a 1 in. diameter lens with a focal length of 1 m. Once the fragment ions are produced, they are accelerated down a 1 m flight tube by a series of three stainless steel plates that have stainless steel mesh across an open center. The plates are arranged in the scheme formulated by Wiley and Mclauren.[22]

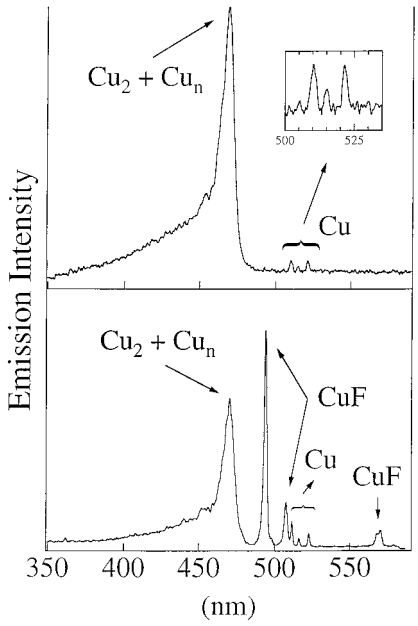


**Figure 1.** (a, top) In-situ luminescence spectrum observed during gas phase 308 nm photolysis at 95 °C of the bis(*tert*-butylacetoacetato)-copper precursor. (b, bottom) In-situ luminescence spectrum observed during gas-phase photolysis of $Cu(hfac)_2$.

Acceleration plate voltages are 3000 V, 2100 V, and ground, respectively in order from furthest to nearest the detector. The flight tube is kept at $10^{-6}$ Torr using a Varian V300HT 6 in. air-cooled turbomolecular pump, and ions are detected using an 18 mm microchannel plate detector assembly. The detector assembly is fitted with two Galileo MCP 18B plates with a 10 $\mu$m channel diameter and a channel spacing of 12.5 $\mu$m. The ion current is processed using a RTD710 Tektronix 200 MHz dual channel digitizer and is monitored on an oscilloscope.

**Photolytic CVD.** Laser driven photodeposition was carried out at ~$10^{-2}$ Torr using a XeCl excimer laser (308 nm). The copper precursor (~0.1 g) in a reservoir cell was heated to its sublimation temperature (95 °C) and introduced into a CVD glass cell with quartz windows with $H_2$ (20 sccm) as a carrier gas. The photodeposition was carried out by 308 nm laser driven decomposition of a gas-phase precursor on substrates (quartz slides) with 30 mJ/pulse at 20 Hz for a resulting fluence of ~1 MW cm$^{-2}$. The shiny films formed exclusively on the irradiated area. Typical growth times were 1 h, and about 0.5 mm thick Cu films were obtained. No attempts were made to optimize the deposition rate.

## Results and Discussion

**1. In-Situ Luminescence during Photolytic CVD.** During the course of the laser-driven CVD studies, we observe luminescence in the path of the laser beam in the cell. The emission spectra show that the luminescence originates from gas-phase photofragments and not from the intact Cu precursor molecule (vide infra). The luminescence provides the opportunity to identify excited photochemical species that are formed during the laser CVD process and to use the information to develop an understanding of the photofragmentation pathways. The luminescence spectrum observed during the deposition process, shown in Figure 1a, exhibits features attributed to metal-containing species and to the free ligand that can be separated by time-resolved gated experiments.[23] Three small lines appear at 510.3, 515.0, and 521.5 nm, within experimental uncertainty of the known Cu emission lines at 510.55, 515.32, and 521.82 nm due to the $^2P^o_{3/2}$ (4p) → $^2D_{5/2}$ (4s$^2$), $^2D_{5/2}$ (4d)

(20) The precursors were prepared by reported methods: (a) Graddon, D. P. J. *Inorg. Nucl. Chem.* **1960**, *14*, 161. (b) Graddon, D. P.; Watton, E. C. J. *Inorg. Nucl. Chem.* **1961**, *21*, 49.
(21) Hwang, S.; Choi, H.; Shim, I. *Chem. Mater*. **1996**, *8*, 981.
(22) Wiley, W. C.; McLaren, I. H. *Rev. Sci. Instrum*. **1955**, *26*, 1150.
(23) The instruments for gas-phase photoluminescence measurements were described in ref 12.

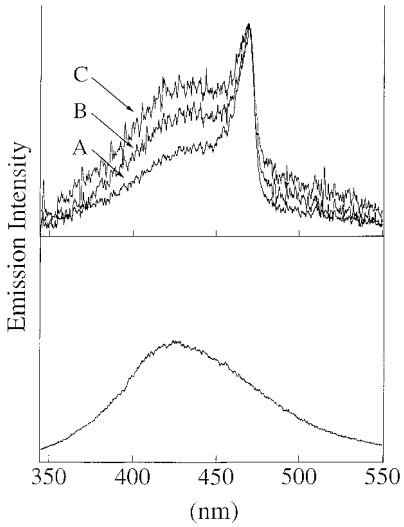


**Figure 2.** In-situ luminescence spectra at 95 °C obtained by time-resolved gating experiments delayed 1.0 $\mu$s after the 308 nm laser pulse and integrated for (A) 3 $\mu$s, (B) 10 $\mu$s, and (C) 70 $\mu$s. The lower trace is the spectrum observed from free *tert*-butylacetoacetate under identical conditions with continuous integration.

$\rightarrow {}^2P^o_{1/2}$ (4p), and ${}^2D_{5/2}$ (4d) $\rightarrow {}^2P^o_{3/2}$ (4p) transitions, respectively (Figure 1, inset).[24,25] The more intense and asymmetric feature at 468 nm includes contribution of $Cu_2$ ($B^1\Pi_u - X^1\Sigma_g^+$) and possibly Cu clusters.[12,26] The formation of metal dimers and clusters has been observed upon gas-phase photolysis of other volatile organometallic compounds.[10,11] In comparison, the emission spectrum obtained from $Cu(hfac)_2$ under the same conditions shows not only the identical asymmetrical broad peak at 468 nm and weaker peaks at 510.3, 515.0, and 521.5 nm of Cu atomic emission but also additional strong peaks at 493.0, 507, and 569.1 nm (Figure 1b). The latter three peaks are from copper fluoride (CuF) diatomic emissions arising from the transitions $C^3\Sigma_1 \rightarrow X^1\Sigma^+$ at 493.5 nm, $B^1\Sigma^+ \rightarrow X^1\Sigma^+$ at 507 nm, and $A^3\Pi_2 \rightarrow X^1\Sigma^+$ at 568.6 nm.[12,27] The spectra obtained during the gas-phase photolysis of $Cu(baa)_2$ show only Cu-containing species and the free ligand while that of $Cu(hfac)_2$ also exhibits CuF emission.

To separate the spectra arising from non-copper-containing species from the spectra involving the copper, gating experiments were carried out. The time-resolved gating experiment (with the gate delayed 1 $\mu$s after the laser pulse) reduces the intensity of the relatively short-lived Cu related emission band at 468 nm and shows a single broad emission band from 350 to 500 nm (Figure 2). As the integration time is increased, the relative intensity of the broad emission band from longer lived species increases as shown in Figure 2a−c. This band is assigned to the $\pi \rightarrow \pi^*$ transition of the free *tert*-butylacetoacetate ligand. The control emission experiment, photoexcitation of the pure *tert*-butylacetoacetate ligand under identical conditions but with continuous integration (no gating), shows a broad asymmetric band with its maximum at about 420 nm (Figure 2, bottom), which reproduces the long-lived emission band shown in the top of Figure 2. These experiments show that the free ligand is present and luminescing, but they do not differentiate between dissociation of an excited ligand or excitation of a ground-state free ligand by subsequent photons.

**2. Time-of-Flight Mass Spectroscopic Analysis of Photofragments.** The generation of free ligand and Cu-containing species is confirmed by the mass spectroscopic experiment. The sublimed Cu precursor is introduced into the TOF chamber ($\sim 10^{-5}$ Torr base pressure) and then both photoexcited and ionized in the supersonic molecular beam by the 308 nm laser pulse. Atomic Cu ($m/z$ = 63 and 65), the monoligand Cu complex $Cu(MeCOCHCOOBu^t)_1$ ($m/z$ = 221), and the bare ligand $MeCOCHCOOBu^t$ ($m/z$ = 157) are observed along with species from the heavily fragmented ligand such as CO ($m/z$ = 28), CHCO ($m/z$ = 41), $CMe_3$ ($m/z$ = 57), and $O-CMe_3$ ($m/z$ = 73) ions. This mass spectroscopic identification of copper, and more importantly of the dissociated species CuL and the intact ligand, is consistent with the luminescence results. The dissociated ligands probably absorb additional photons and undergo further photofragmentation to give the various low mass species.

The production of Cu metal atoms in the gas phase involves multiple ligand dissociations.[28] There have been reports on analogous photoactivated ligand dissociation processes for copper acetate complexes that involve homolytic cleavage of the M−O bond.[1,29] Similarly, the production of Cu from bis-(acetylacetonate)copper complexes by the direct loss of both of the acetylacetonate ligands has been studied by using the multiphoton dissociation/ionization technique.[30] The luminescence of the metal atoms probably occurs because they are produced in excited electronic states. Copper atoms do not have an absorption band at 308 nm.[24]

The generation of Cu dimers and clusters is facilitated by the relatively high concentration and collision conditions in the 6-way cross experiment (total pressure $\sim$ 0.1 Torr), while, under the cold and collision free conditions in the molecular beam, dimers and clusters are not formed. Both the in-situ luminescence under deposition conditions and the mass spectroscopy of the precursor in the molecular beam clearly prove that metal atoms (and ions) are produced and that complete ligand dissociation occurs as a result of the gas-phase photochemistry.

**3. Laser Driven Photochemical Synthesis of Cu Deposits and Film Properties.** The spectroscopic identification of the photofragments described above shows only homolytic Cu, Cu dimers, and perhaps larger clusters and does not show any diatomic molecules containing Cu and heteroatoms. To check the correlation between our spectroscopic observation of gas-phase species and the solid-state materials, we examine our deposits and the purity of the materials. It is important to verify the film is also pure and does not contain any heteroatoms.

Laser driven photodeposition was performed using 308 nm light. The precursor ($\sim$0.1 g) in a reservoir cell under vacuum ($10^{-1}$ Torr) was heated to its sublimation temperature and introduced into a CVD glass cell with quartz windows using $H_2$ as carrier gas. The photodeposition of Cu was carried out on quartz slide substrates with pulse energies of 30 mJ/pulse at

(24) Striganov, A. R.; Sventitskii, N. S. *Tables of Spectral Lines of Neutral and Ionized Atoms*; IFI/Plenum: New York, 1968.
(25) Moore, C. E. *Atomic Energy Levels*; National Bureau of Standards: Washington, DC, 1952; Vol. II.
(26) A similar broad feature is observed by ablating copper foil under similar conditions, leading to the conclusion that this feature is due at least in part to $Cu_n$. Also, an identical feature is observed in the spectra obtained during the photolysis of $Cu(hfac)_2$ in a gas cell in ref 12.
(27) Pease, R. W. B.; Gaydon, A. G. *The Identification of Molecular Spectra*, 3rd ed.; Chapman and Hall: London, 1976.
(28) The fragmentation pattern of the precursor from 70 eV electron impact mass analysis identifies the Cu atom, molecular ion, Cu complex with one ligand $Cu(MeCOCHCOOBu^t)$, dimer $Cu_2(MeCOCHCOOBu^t)_4$, three ligand bimetallic species $[Cu_2(MeCOCHCOOBu^t)_3]$, and a *tert*-butylacetoacetate ligand as major species. This also indicates that facile Cu−O bond cleavage occurs.
(29) Balzani, V. *Photochemistry of Coordination Compounds*; Academic: New York, 1970; p 270.
(30) Mikami, N.; Ohki, R.; Kido, H. *Chem. Phys.* **1990**, *141*, 431.

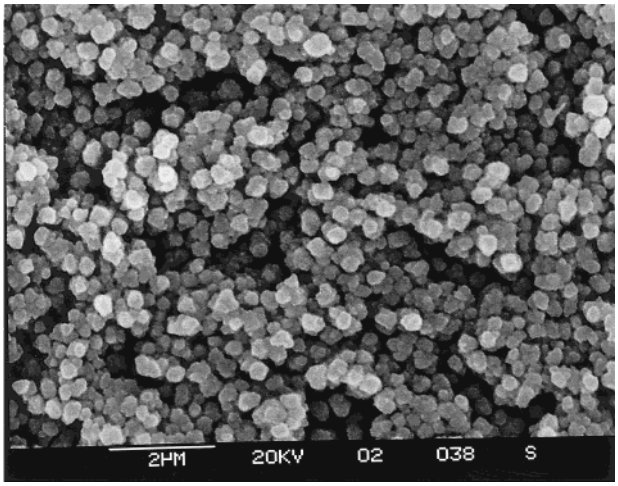


**Figure 3.** SEM image of the Cu deposits grown on quartz by photochemical vapor synthesis.

20 Hz with a resulting fluence of ~1 MW $cm^{-2}$. Typical deposition times were about 1 h, and ~500 nm thick deposits were obtained.

Scanning electron microscopy (SEM) images show that the Cu deposits consist of uniform particles (~200 nm in diameter) (Figure 3). Similar homogeneous particle formation in the deposits have been observed during laser-induced CVD of thin films by us and others.[31,32] In contrast, larger grain formation results from pyrolytic CVD.[21] It is possible that, during the photolytic process, nucleation seeds are formed in the gas phase that facilitate further growth into clusters and particles.

X-ray diffraction (XRD) patterns of the films show that the particles are polycrystalline Cu with (111) and (200) peaks at $2\theta$ of 43.3 and 50.2°, respectively.[33] The purity of these Cu particles was examined by X-ray photoelectron spectroscopic (XPS) and energy-dispersive X-ray spectrometric (EDS) analyses. The XPS analysis of the unsputtered sample shows that surface is oxidized and contaminated with carbon from the atmosphere. Figure 4a shows the Cu 2p region; peaks due to copper oxide are observed on the surface.[34] Subsequent $Ar^+$ ion sputtering of the surface removes the oxide layer and peaks due to pure Cu $2p_{3/2}$ and $2p_{1/2}$ are observed at 932.5 and 952.3 eV, respectively (Figure 4b).[34] The binding energies in the 2p region show that Cu(O) is formed rather than copper in a higher oxidation state.[34] The carbon and oxygen content decreases to near the detection limit level (~1%). EDS analysis on a small region (~1 $\mu$m × 1 $\mu$m) also confirms the presence of Cu without any other contaminants. According to our analysis, pure and uniform spherical Cu particles are obtained from the photolytic processes. The photolytic generation of Cu clusters,

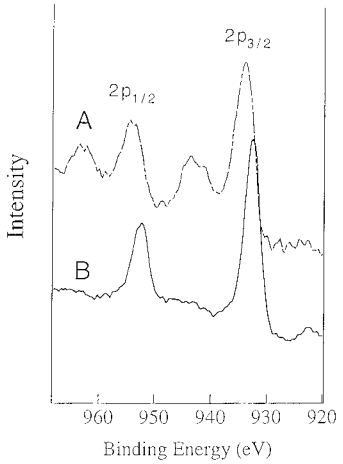


**Figure 4.** XPS of a Cu film grown on quartz by photochemical CVD in the 2p region: (a) unsputtered film; (b) after 7 min of $Ar^+$ sputtering.

Cu dimer, and Cu atoms occurs in the gas phase as shown by our spectroscopic studies, and it is possible that the subsequent aggregation of these clusters to form particles may also occur in the gas phase. Surface reactions probably play a role, but the morphological differences between the pyrolytic and photolytic deposits, and the proof that copper atoms and the beginnings of aggregation occur in the gas phase, show that laser CVD is more than just a method of locally heating the substrate. Similar spectroscopic identification of gas-phase diatomic intermediates and solid-phase bulk materials with the same stoichiometry have been observed in the case of metal nitride by us.[35]

## Summary

The in-situ gas-phase luminescence measurements show that Cu atoms, Cu dimers, and free ligands are the major luminescent species present during photodeposition under low vacuum (~$10^{-1}$ Torr) CVD conditions. Under higher vacuum conditions (~$10^{-5}$ Torr) in a molecular beam, Cu atoms, dissociated ligands, and partially deligated complexes are observed by TOF mass spectroscopy. The nucleation of Cu atoms to form dimers is observed under CVD conditions, and pure polycrystalline Cu particles are deposited. The results show that there is a significant contribution of a gas-phase photolytic component to the laser CVD. The use of a laser as a tool for both the preparation of materials and for the identification of intermediates is a general method that can be utilized for both mechanistic studies and materials synthesis.

**Acknowledgment.** This work was supported by the National Science Foundation (Grant CHE-9816552 for J.I.Z.) and KOSEF (Grant 1999-1-122-001-5 for J.C.). We thank Gary Rose (UCLA) for assistance with the XPS analyses and Peter Muraoka for assistance with the mass spectroscopy.

IC990962A

(31) Dupuy, C. G.; Beach, D. B.; Hurst, J. E., Jr.; Jasinski, J. M. *Chem. Mater*. **1989**, *1*, 16.
(32) Unpublished results, J. Cheon and J. I. Zink. Homogeneous Pd particles are obtained from laser CVD of Pd organometallics.
(33) *JCPDS Powder Diffraction File*; McClune, W. F., Ed.; International Center for Diffraction Data: Swarthmore, PA, 1990.
(34) *Handbook of X-ray Photoelectron Spectroscopy*; Muilenberg, G. E., Ed.; Perkin-Elmer: Eden Prarie, MN, 1978.
(35) Cheon, J.; Guile M.; Muraoka, P.; Zink, J. I. *Inorg. Chem*. **1999**, *38*, 2838